CONFERENCE PRE-PRINT

ANALYSIS AND SIMULATION OF EFFECTIVE RUNAWAY ELECTRON MITIGATION USING A PASSIVE COIL IN J-TEXT DISRUPTIONS

CHANG LIU, QIHANG LI
State Key Laboratory of Nuclear Physics and Technology, School of Physics, Peking University, Beijing 100871, China
Email: changliu@pku.edu.cn

JUNHUI YANG, ZHONGHE JIANG, NENGCHAO WANG
Huazhong University of Science and Technology, Wuhan, Hubei 430074, China

STEPHEN C. JARDIN, NATHANIEL M. FERRARO
Princeton Plasma Physics Laboratory, Princeton, NJ 08540, USA

Abstract

Disruptions and runaway electrons (REs) pose a significant challenge to the safety and stability of tokamak-based fusion reactors. Recently, a passive coil method for RE mitigation has been tested in the J-TEXT tokamak, achieving complete suppression of the RE current plateau. In this work, we present a self-consistent simulation of this RE suppression using the M3D-C1 code. The results align with experimental findings, including plasma and coil current evolution and RE current suppression. Analysis of the simulation indicates that RE current generated near the magnetic axis plays a crucial role in sustaining peak current profile and maintaining the q=2 rational surface, which is essential for MHD instability excitation and magnetic field stochasticization. The passive coil plays a supporting role by providing seed magnetic perturbation and facilitating MHD mode growth. This study highlights the importance of incorporating RE current and its interaction with MHD instabilities when evaluating the effectiveness of the runaway electron mitigation coil (REMC).

1. INTRODUCTION

One of the central challenges in ensuring the safe operation of tokamak devices is the prevention and mitigation of high-energy runaway electron (RE) beams generated during major disruptions. For high-current machines such as ITER, theoretical studies predict that the avalanche process—initiated by knock-on collisions between an energetic seed electron and a thermal electron—can amplify the RE population by up to ten orders of magnitude [1]. Seed electrons may arise from the acceleration of the hot-electron tail or from tritium beta decay within the plasma. This exponential growth can cause REs to carry a substantial fraction of the plasma current, forming a beam-like RE current surrounded by a halo plasma. If uncontrolled, the beam can strike the vessel wall during the final loss phase, leading to melting of plasma-facing components (PFCs) and damage to internal cooling channels. Such RE-induced melting has already been observed in devices including JET and WEST. Consequently, the development of reliable RE mitigation strategies is essential for the safe operation of future tokamak reactors.

The most effective RE mitigation strategy developed to date is the injection of massive impurities into the plasma during the thermal quench (TQ) phase of a disruption. This approach increases plasma collisionality and facilitates the diffusion of seed REs during the TQ. It has been successfully demonstrated in several existing tokamak devices and has been selected as the primary disruption mitigation method for ITER. However, self-consistent fluid simulations with the DREAM code indicate that [2], due to seed REs generated by tritium decay and the large avalanche multiplication factor, this technique cannot fully prevent the formation of mega-ampere–level RE currents, which remain unacceptable for ITER operation. An alternative approach seeks to enhance RE diffusion during the current quench (CQ) phase. This can be achieved by exciting instabilities driven by the free energy of REs, including Alfvén-wave and magnetohydrodynamic (MHD) instabilities. The central idea is to introduce strong magnetic perturbations, or even magnetic field stochastization, during the CQ to amplify RE transport and losses sufficiently to counter avalanche growth. Given the high risks associated with uncontrolled RE beams, the efficacy of these mitigation strategies must be rigorously validated through dedicated experiments and advanced numerical modeling.

Another proposed approach for RE mitigation is the introduction of magnetic perturbations via external coils. The use of resonant magnetic perturbation (RMP) coils for RE beam control has been investigated through test-particle simulations [3]. A potentially more effective strategy employs passive coils with non-axisymmetric geometry, in which currents are induced by the loop voltage generated during the rapid drop of plasma current [4]. Unlike active RMP systems, passive coils respond spontaneously to a CQ and can sustain coil currents significantly larger than those typically achieved with RMP coils. Previous MHD simulations incorporating test-particle RE models have demonstrated that passive coils can effectively suppress RE growth in the early stages of the CQ [5]. Owing to this promise, passive coils have been adopted as a key component of the disruption mitigation systems planned for SPARC and STEP tokamaks. Nevertheless, recent simulations suggest that in the later phase of the CQ, closed flux surfaces may re-form near the plasma core, providing a potential reservoir for avalanche-driven RE amplification [6].

Recently, passive-coil–based RE mitigation has been tested experimentally for the first time in a tokamak. The J-TEXT team installed a helical coil inside the first wall of their circular tokamak to evaluate its ability to generate magnetic perturbations and suppress RE growth. The experiments clearly demonstrated the effectiveness of the passive coil in preventing the formation of a post-CQ RE plateau. As shown in Fig. 1, activating the passive coil reduced the pre-disruption electron density threshold required for plateau suppression. Furthermore, analysis of plasma current and hard X-ray time traces—which serve as indicators of RE loss—revealed that, with the passive coil engaged, REs underwent more frequent and sustained loss events during the CQ. This provides strong experimental evidence of the coil's mitigation effect.

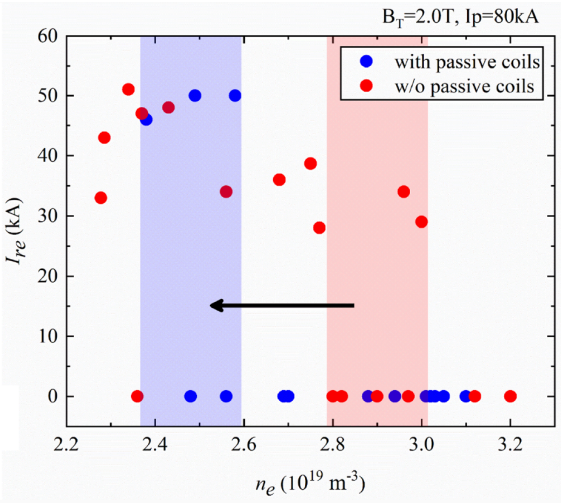

Fig. 1 Summary of final RE plateau level of multiple J-TEXT disruption experiments under varying pre-disruption electron densities and passive coil conditions.

Despite the encouraging experimental results, initial attempts to reproduce the findings through simulations have faced difficulties. Unlike conventional RMP coils, the helical passive coil generates magnetic perturbations with a narrow spectrum in both toroidal and poloidal mode numbers. Such perturbations fail to produce strong resonances with the tokamak magnetic field when the on-axis safety factor, q_0, is significantly greater than unity. Test-particle simulations of REs incorporating only the narrow-spectrum perturbations from the coil confirmed that RE transport was only marginally enhanced compared with the unperturbed case, leading to a clear discrepancy with experimental observations.

On the other hand, the magnetic perturbations observed in the J-TEXT experiments exhibit a broad spectrum, resembling those typically generated by RMP coils. This discrepancy motivated the search for additional mechanisms that could enhance magnetic perturbations, drive RE losses, and clarify their connection to the passive coil. In this work, we employ the 3D MHD code M3D-C1 to simulate the J-TEXT CQ in the presence of the passive coil. Unlike earlier test-particle–based studies, our approach incorporates the feedback of RE current on the MHD equilibrium and the excitation of MHD instabilities. This is achieved through a self-consistent fluid RE model that includes RE avalanche growth. The passive coil is represented using the resistive wall module in M3D-C1 by introducing a low-resistivity channel in the 3D mesh outside the plasma. Simulation results demonstrate that, during the CQ, the passive coil can trigger strong MHD instabilities, and that magnetic islands

arising from these instabilities play the dominant role in RE losses. The details of the simulation model and the underlying physics of the RE–coil–MHD interaction are presented in the following sections.

2. SIMULATION MODEL

2.1. FLUID MODEL OF RUNAWAY ELECTRONS IN M3D-C1

The M3D-C1 code [7] is an implicit extended magnetohydrodynamic (MHD) solver that employs high-order, C^1-continuous finite elements in three dimensions. In the (R,Z) plane, the code uses an unstructured triangular mesh, which is extruded in the toroidal direction to generate structured triangular prism elements for nonlinear 3D simulations. This flexible meshing strategy allows localized refinement, enabling high spatial resolution near rational surfaces or other regions where strong gradients are expected to develop.

To investigate the self-consistent interaction between RE current and MHD instabilities during disruptions, a fluid RE model has been implemented in M3D-C1 [8], similar to those employed in other MHD codes such as M3D-K, NIMROD, JOREK, and EXTREM. In this model, the RE density evolves according to an advection equation that includes the parallel velocity and the E×B drift, while other drift terms are neglected. The RE current is then derived from the density under the assumption that relativistic RE motion is dominated by parallel streaming at the speed of light, with additional contributions from the E×B drift. This calculated RE current is self-consistently coupled into the momentum equation and the Ohm's law. The governing fluid RE model is summarized by the following set of equations:

$$\frac{\partial n_{RE}}{\partial t} + \nabla \cdot \left[n_{RE} \left(v_{\parallel} \mathbf{b} + \frac{\mathbf{E} \times \mathbf{B}}{B^2} \right) \right] = S$$

$$\mathbf{J}_{RE} = -e n_{RE} (c\mathbf{b} + \frac{\mathbf{E} \times \mathbf{B}}{B^2})$$

$$nm \left[\frac{\partial \mathbf{V}}{\partial t} + (\mathbf{V} \cdot \nabla) \mathbf{V} \right] = e n_{RE} \mathbf{E} + (\mathbf{J} - \mathbf{J}_{RE}) \times \mathbf{B} - \nabla p$$

$$\mathbf{E} + \mathbf{v} \times \mathbf{B} = \eta (\nabla \times \mathbf{B} - \mathbf{J}_{RE})$$

Compared with kinetic models, the fluid RE model offers a substantial simplification of RE–MHD coupling computations. However, it cannot capture important effects such as RE orbit deviations from flux surfaces due to curvature drifts, or resonances between RE motion and plasma instabilities. Moreover, it does not provide accurate predictions of RE growth or decay, as this would require detailed knowledge of the momentum-space distribution of REs. Instead, analytical expressions for RE growth, including avalanche effects, are incorporated. In modeling avalanche growth, we account for the contribution of bound electrons from partially ionized argon, which is injected to trigger the disruption. The model includes both the enhancement of avalanche multiplication due to additional background electrons and the reduction caused by partial nuclear screening, following the set of equations derived in [9].

2.2. PASSIVE COIL MODELING IN M3D-C1

M3D-C1 includes an option for realistic free-boundary MHD simulations. In this mode, a multi-region finite element mesh is employed, covering the plasma, the resistive wall, and the surrounding vacuum. Within the resistive wall region, a reduced set of equations is solved, consisting only of Maxwell's equations (without the displacement current) and Ohm's law. In practice, this means that Maxwell's equations are evolved consistently across the entire domain, while the current evolution is treated differently in each region. Under this framework, magnetic fields from external coils can be incorporated either by explicitly including coil currents within the simulation domain or by imposing boundary conditions to represent external magnetic fields.

For the J-TEXT simulations, we adopt the first approach of explicitly including the coil current within the simulation domain. The coil current can either be prescribed using a predefined time-dependent profile or computed self-consistently by solving Maxwell's equations. In the latter case, we employ the resistive wall module of M3D-C1 to construct a virtual resistive shell outside the circular plasma, assigning it a large resistivity to suppress wall currents. A thin, low-resistivity helical channel is then carved into this shell,

following the geometry of the J-TEXT passive coil (Fig. 2). This configuration guides the induced wall current along the helical channel, thereby generating the corresponding magnetic perturbations inside the plasma.

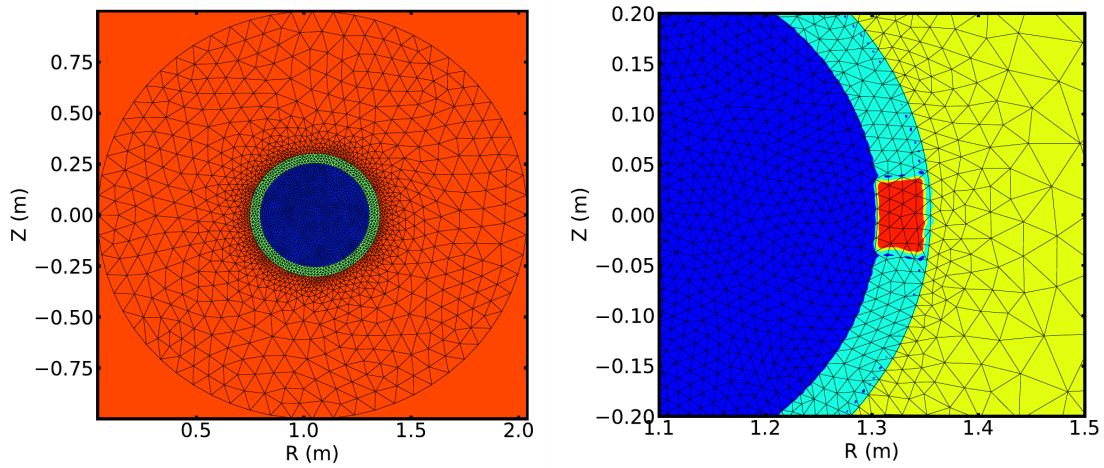

Fig. 2 Multi-region mesh used in the M3D-C1 simulation of the J-TEXT passive coil. (Left) Blue, green, and red denote the plasma, wall, and vacuum regions, respectively. (Right) The red region indicates the low-resistivity channel embedded within the resistive wall.

The passive coil module in M3D-C1 was first validated using a simplified CQ simulation without RE generation. The time evolution of the total plasma current and the induced coil current is shown in Fig. 3. During the CQ, the coil current grows approximately linearly and saturates near the end of the quench, reaching a value about 10% of the initial plasma current. This saturation level is consistent with J-TEXT experimental observations. Parameter scans further indicate that the saturation current is constrained by both the coil resistivity and the spatial resolution of the simulation mesh. In addition, we computed the magnetic perturbation spectrum induced by the coil in the plasma region. As shown in Fig. 3, the perturbed field contains a dominant n=1 component along with higher harmonics, in agreement with previous Biot–Savart calculations of the coil field.

Several numerical challenges have been encountered in the passive coil simulations. Accurately modeling the thin current channel requires high toroidal mesh resolution, exceeding what is typically necessary to resolve the MHD modes excited during the CQ. In addition, a large vacuum region must be included outside the resistive wall to mitigate boundary-condition effects on the coil current. These requirements significantly increase computational costs. To address this, future work will employ more flexible finite-element tools such as COMSOL and ThinCurr to model the passive coil current and couple it with M3D-C1 MHD simulations, thereby reducing computational expense.

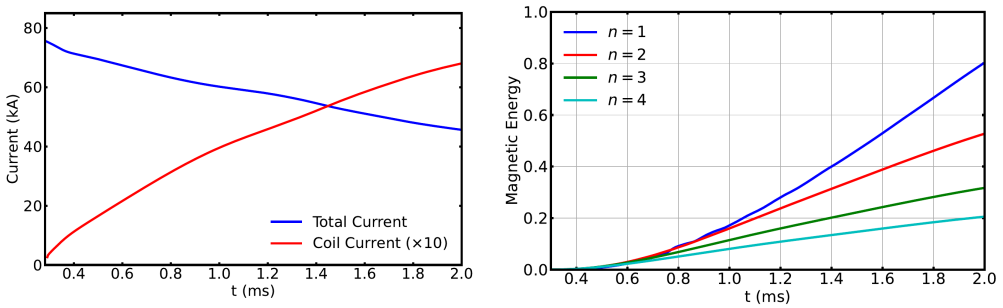

Fig. 3 Test simulation of passive coil current excitation in J-TEXT. (Left) Growth of coil current (red) during the plasma current (blue) quench. (Right) Increase of the magnetic field energy associated with perturbations from passive coils.

3. CURRENT QUENCH SIMULATION USING M3D-C1

3.1. 2D SIMULATION WITH RE CURRENT

We first performed axisymmetric MHD simulations of the CQ with RE current, excluding any external coil effects. In typical J-TEXT disruptions, the relatively low initial plasma current yields a total RE amplification factor of only 2–3, as estimated by the Rosenbluth–Putvinski avalanche rate. Contributions from bound electrons can provide an additional factor of ~2. Consequently, the CQ simulation should begin with an initial RE current of about 20% of the experimentally observed RE plateau, serving as the seed for avalanche growth. Such seed REs may originate either from pre-disruption low-density discharges or from hot-tail generation during TQ. Given the strong MHD activity and field stochasticity during the TQ, it is expected that seed REs can only survive on the remaining closed flux surfaces near the magnetic axis. Accordingly, we initialize the RE current with a peaked profile centered on the axis, corresponding to ~10% of the total plasma current.

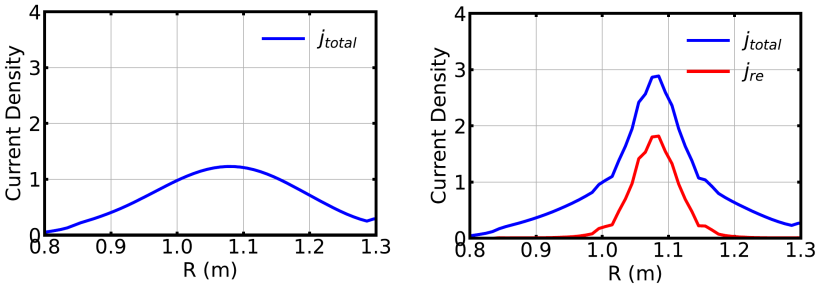

Fig. 4 Total and RE current relaxation in 2D CQ simulation. (Left) In the absence of RE current present, the Ohmic current profile flattens during the CQ. (Right) In presence of RE current, the total plasma current remains peaked.

Following the TQ, the plasma temperature drops significantly, leading to high resistivity, with the Lundquist number reduced to ~10^4. In the absence of RE current, this elevated resistivity causes rapid diffusion of the plasma current and relaxation of the current profile, as shown in Fig. 4. When RE current is included in the MHD model, however, the total current profile becomes more peaked during CQ. As indicated by the MHD equations with RE current, the RE contribution is unaffected by resistivity and associated spatial diffusion. Moreover, avalanche growth further sharpens the RE profile during the CQ. As illustrated in Fig. 4, the central RE current helps support a strongly peaked total current profile.

The difference in current profile evolution has a strong impact on MHD mode behavior during the CQ. Fig. 5 shows the time evolution of the on-axis safety factor (q_0) from 2D simulations with and without RE current. The initial q_0 is close to unity, consistent with induction-driven Ohmic current prior to disruption. In the case without RE current, q_0 rises rapidly due to current profile relaxation. By contrast, the presence of a peaked RE current maintains q_0 near 1.5 throughout the CQ. This peaked profile increases plasma susceptibility to current-driven MHD modes by enhancing current gradients near rational surfaces. Furthermore, the lower q_0 strengthens resonance with the passive coil, since the coil perturbation spectrum is concentrated near m=n.

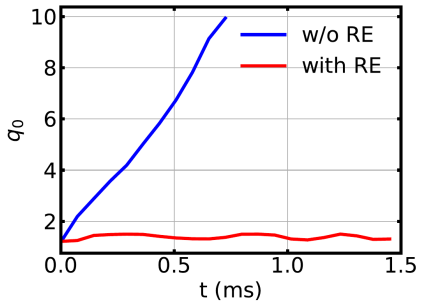

Fig. 5 Time evolution of on-axis q value in 2D CQ simulation, without RE current (blue) and with RE current (red).

3.2. 3D SIMULATION WITH RE CURRENT AND PASSIVE COIL

Building on the 2D results, we performed a series of 3D nonlinear simulations with the passive coil activated to investigate the excitation of MHD instabilities and their interaction with the coil. For a typical case, the computational mesh consisted of 32 toroidal planes with ~6000 triangular elements per plane. A large dissipation term was introduced in the temperature equation to represent strong impurity radiation in the post-TQ plasma, thereby constraining the plasma temperature to a low level and yielding high resistivity. At the

start of the simulation, a peaked RE current profile corresponding to ~10% of the total plasma current was initialized, consistent with the setup described in Sec. 3.1.

The time evolution of the RE current profile and magnetic fields is summarized in Fig. 6. Initially, avalanche-driven RE growth produces a strongly peaked total current profile, as described in Sec. 3.1. When the steep current gradient overlaps the q=2 flux surface, a (2,1) tearing mode is excited, leading to rapid island growth. This in turn drives fast RE transport along perturbed magnetic field lines, flattening the RE profile near the q=2 surface and subsequently damping the (2,1) mode. The redistributed REs then form a new front at larger radii, creating another steep gradient. When this front intersects the q=3 surface, a (3,1) tearing mode is triggered, producing similar rapid transport and profile flattening within ~0.1 ms. This process repeats sequentially, with tearing modes excited at progressively higher m. At later times, multiple modes coexist, causing island overlap and magnetic field stochastization. Nonetheless, RE transport remains dominated by X-point dynamics, while expanding islands form hollow regions in the RE current distribution. Ultimately, this cascade of tearing mode excitation drives RE transport from the core toward the edge, flattening both the RE and total current profiles and raising q_0. Meanwhile, the magnetic axis shifts toward the high-field side as the total current decreases. The combination of wall contact and tearing-mode activity provides an effective channel for RE losses.

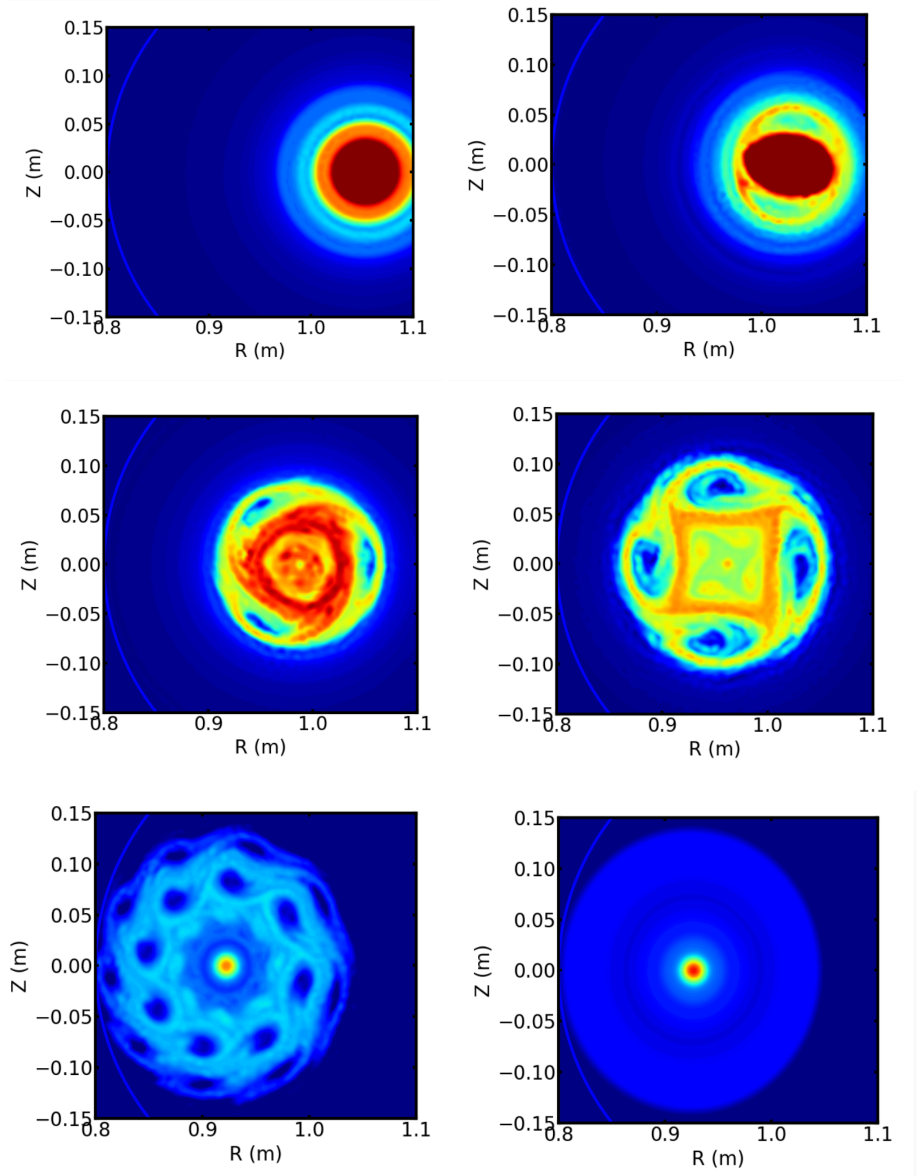

Fig. 6 RE density evolution during 3D CQ simulation with passive coil turned on. The six plots show the RE density at t=0.22ms, 0.29ms, 0.44ms, 0.58ms, 1.015ms and 1.596ms, respectively.

A detailed analysis of magnetic perturbations during the CQ simulation was performed. Fig. 7 shows the Schaffer plot of the n=1 perturbed field spectrum. Unlike the perturbations generated by RMP coils or runaway electron mitigation coils designed for other tokamaks, the helical coil produces only an m=1 perturbation, which appears as the vertical line in Fig. 7. This perturbation does not intersect resonant flux surfaces (indicated by the blue dashed line). Instead, the bright spots in the Schaffer plot that do overlap with the resonant line correspond to the dominant MHD modes excited at that time. These bright spots migrate outward, reflecting the transition of dominant modes from low-m to high-m. Eventually, the spectrum quiets, leaving only the persistent m=1 perturbation from the helical coil. At this stage, although the passive coil current reaches its maximum, it alone cannot generate magnetic islands due to the absence of resonances, and the flux surfaces return to a closed, regular configuration.

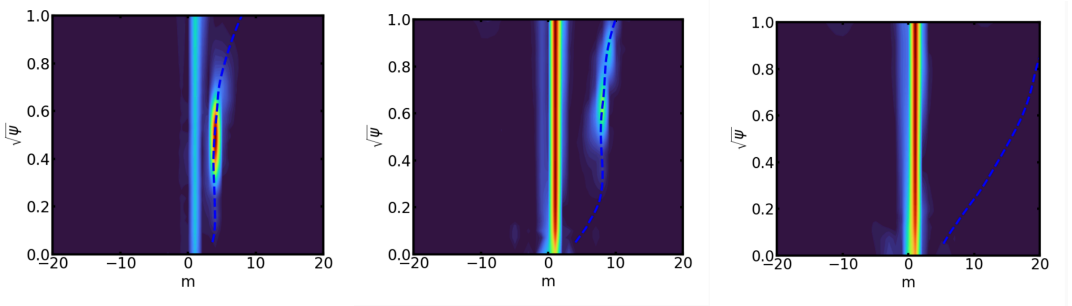

Fig. 7 Schaffer plot of n=1 magnetic field perturbation at t=0.58ms, 1.015ms and 1.596ms. The blue dashed line represents the resonant modes satisfying m/n=q.

The above analysis suggests that the helical passive coil is not directly responsible for field stochastization or RE losses during the CQ, owing to the absence of resonances with rational surfaces. However, the coil can provide sidebands of the dominant m=n perturbations, effectively acting as seeds for MHD instabilities. This effect is particularly important in the early CQ phase, when q_0 remains close to unity. Although not directly visible in the Schaffer plot, the influence can be demonstrated by comparing 3D simulations with and without the passive coil. As shown in Fig. 8, activating the coil leads to larger MHD mode amplitudes than in the no-coil case. The difference is especially pronounced at high plasma viscosity. In this regime, the MHD mode amplitude without the coil is several orders of magnitude smaller than in low-viscosity plasmas, whereas with the coil, the amplitudes are comparable across both viscosity cases. High viscosity strongly reduces the linear growth rate of tearing modes, so magnetic islands require longer times to grow and may fail to produce significant transport before the q-profile evolves. By seeding perturbations, the passive coil raises the initial island amplitude and shortens the growth time needed to trigger transport. Since post-CQ plasmas typically exhibit high viscosity due to low temperatures and strong collisionality, the helical coil can indeed play a critical role in initiating RE losses.

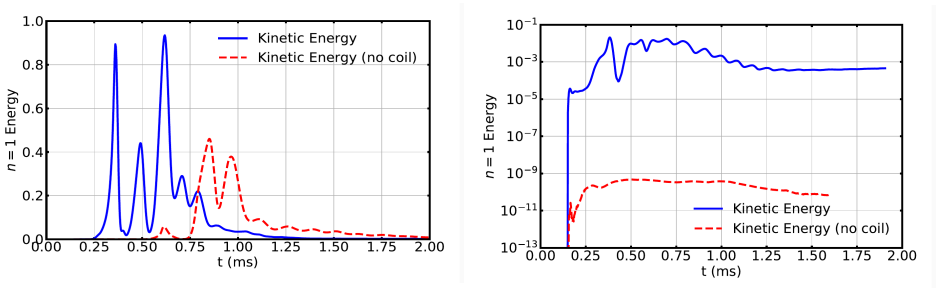

Fig. 8 Kinetic energy of MHD mode from 3D simulation, without (red) and with (blue) passive coil. The left plot shows the results with small plasma viscosity, and the right plot shows the result with significant viscosity.

As a consequence of RE losses, the passive coil and the MHD instabilities it triggers can substantially reduce the final RE current. As shown in Fig. 9, when the passive coil is included, the excitation of MHD modes during the CQ leads to a continuous decrease in RE current and, correspondingly, a steady decline in the total plasma current. In contrast, in CQ simulations without the coil, MHD activity is minimal, allowing the RE current to grow to a higher saturation level and form a post-CQ RE plateau—consistent with experimental observations when the coil is turned off.

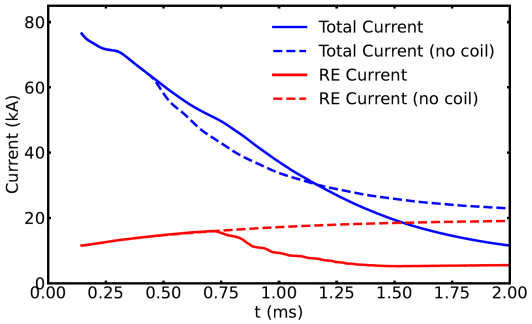

Fig. 9 Time evolution of RE current and total plasma current in simulations: case without passive coil (dashed) versus case with passive coil and MHD instabilities (solid).

4. CONCLUSIONS

In this work, we carried out self-consistent MHD simulations of the J-TEXT current quench with a passive helical coil, including the feedback of RE current on MHD mode excitation. The simulations demonstrated that MHD activity can induce field stochasticity near the X-point, creating a channel for RE transport from the core to the edge. The presence of RE current helps sustain a peaked current profile and a sheared q profile, which in turn facilitates the excitation of successive tearing modes. The passive coil plays a complementary role by providing seed magnetic perturbations that shorten the island growth time needed to drive strong RE diffusion. By varying plasma viscosity, the nonlinear simulations successfully reproduced the divergent outcomes of RE plateau formation with and without the helical coil. Moreover, the simulated MHD mode activity—diagnosable in experiments via Mirnov coils—shows distinct differences between discharges with the passive coil engaged and disengaged. A more detailed analysis of experimental MHD mode behavior and comparisons with simulations will be presented in future work.

In this study, we did not perform a parameter scan of pre-disruption plasma density, which can strongly influence the initial RE seed level. Such a scan is essential to explain the variation in RE plateau levels observed in Fig. 1. Furthermore, the bifurcated behavior of the plateau suggests a competition between RE current and MHD instabilities: higher RE current may suppress MHD activity, providing positive feedback that enhances RE growth. This behavior was not reproduced in our simulations, indicating that a more detailed investigation of the role of RE current in MHD mode excitation is needed to account for these observations.

ACKNOWLEDGEMENTS

This work was supported by The Fundamental Research Funds for the Central Universities, Peking University.

REFERENCES

[1] Boozer, A. H., “Pivotal issues on relativistic electrons in ITER”, Nucl. Fusion 58, 036006 (2018)
[2] Vallhagen, O., et al., “Runaway electron dynamics in ITER disruptions with shattered pellet injections,” Nucl. Fusion 64(8), 086033 (2024).
[3] Papp, G., et al., “Runaway electron losses caused by resonant magnetic perturbations in ITER,” Plasma Phys. Control. Fusion 53(9), 095004 (2011).
[4] Smith, H. M., et al., “Passive runaway electron suppression in tokamak disruptions,” Phys. Plasmas 20(7), 072505 (2013).

[5] Tinguely, R. A., et al., “Modeling the complete prevention of disruption-generated runaway electron beam formation with a passive 3D coil in SPARC,” Nucl. Fusion 61(12), 124003 (2021).
[6] Izzo, V. A., et al., “Disruption mitigation modeling for the SPARC tokamak”, Physics of Plasmas 32(4), 042507 (2025).
[7] Jardin, S. C., et al., “Multiple timescale calculations of sawteeth and other global macroscopic dynamics of tokamak plasmas,” Comput. Sci. Disc. 5(1), 014002 (2012).
[8] Zhao, C., et al., “Simulation of MHD instabilities with fluid runaway electron model in M3D-C 1,” Nucl. Fusion 60(12), 126017 (2020).
[9] Hesslow, L., et al., “Influence of massive material injection on avalanche runaway generation during tokamak disruptions,” Nucl. Fusion 59(8), 084004 (2019).